.

LIMITED VIEW RESOLVING POWER OF CONDUCTIVITY IMAGING FROM BOUNDARY MEASUREMENTS

HABIB AMMARI, JOSSELIN GARNIER, AND KNUT SØLNA

Abstract. In this paper we consider resolution estimates for a linearized inverse conductivity problem with limited-view data. Our purpose is to precisely describe the effect of the limited-view aspect on the resolving power of the measurements in the presence of measurement noise. We first show that, in the shallow probing regime, where the inclusion is close to the boundary of the background medium, we can resolve for any signal-to-noise ratio a sufficiently shallow perimeter perturbation of a conductivity inclusion on the overlap of the source and receiver apertures. Then we provide explicit formulas for the modes that can be resolved and the resolution measure for a given signal-to-noise ratio in the deep probing regime, where the radius of the inclusion is small.

1. Introduction

This paper is the continuation of [6] where we have introduced for the first time the notion of resolution in solving the inverse conductivity problem with measurement noise in the full aperture case. The problem is to image inclusions in a background medium from boundary measurements. It lays a mathematical foundation to electrical impedance tomography, which is a method of imaging the interior of a body by measurements of current flows and voltages on its surface. On the surface one prescribes current sources (such as electrodes) and measures voltage (or vice versa) for some or all positions of these sources. The same mathematical model works in a variety of applications, such as breast cancer imaging [9, 23] and mine detection [16].

In [6] we have indeed shown that on the one hand, we have "infinite resolution" in the near-field limit and on the other hand, the relative resolution decreases rapidly with the "depth" of the conductivity inclusion. We have also given estimates for the sensitivity of the linearized inverse conductivity problem to noise.

Our main objective here is to go further and precisely describe the effect of the limited-view aspect on the resolving power of the noisy measurements. We consider here imaging of a perturbed disk-shaped inclusion in the conductivity case. We impose non zero currents on part of a background medium (a concentric disk) containing the perturbed disk and collect the boundary voltage perturbations on another (possibly the same) part of the boundary. We distinguish two important regimes: the shallow probing regime (also called the near-field regime), where the inclusion is close to the boundary and the deep probing regime, where the radius of the inclusion goes to zero.

2000 *Mathematics Subject Classification.* 35R30, 35B30.

Key words and phrases. Imaging, resolution, inverse conductivity problem, instrument noise, partial aperture.

This work was supported by the ERC Advanced Grant Project MULTIMOD–267184.

We first observe that the data in the limited-view case can be expressed as a function of the data in the full-view case using source and receiver filters. We then show that, in the shallow probing regime, we can resolve for any signal-to-noise ratio a sufficiently shallow perimeter perturbation of a conductivity inclusion on the overlap of the source and receiver apertures. Therefore, we have in this case "infinite resolution" on the overlap of the source and receiver apertures. In the deep probing regime, *i.e.*, when the radius of the inclusion is small, we provide a constraint on the number of modes that can be estimated for a given signal-to-noise ratio (SNR). For doing so, we use a filtering approach. Because of the limited-view configuration, it is in general critical to use an inverse filter with off-diagonal terms. We use a matrix filter to estimate the lowest modes of the perimeter perturbation in the situation with a small inclusion. We also show that the estimations of the high modes are more sensitive to measurement noise than those of the low modes.

In connection with our results, we refer in particular to the works by Isakov [19], Ide *et al.* [17], and Alessandrini and Di Cristo [3] on reconstructing conductivity inclusions. For further discussions on the stability of the inverse conductivity problem, see for instance, [2, 9, 10, 12, 13, 20]. As far as we know, our formulas for the resolving power of limited-view measurements in terms of the SNR are new. They provide a deep understanding of the ill-posed nature of the inverse conductivity problem and precisely quantify the effect of the limited-view aspect on the quality of the reconstructed conductivity images. Recently, there has been a lot of work done on the inverse conductivity problem in the limited-view case [15, 22, 18, 24]. Our results also clarify the connection between the full- and the limited-view cases.

The paper is organized as follows. In section 2 we formulate the reconstruction problem of interest. Our goal is to estimate the shape perturbations of a disk-shaped inclusion from limited-view boundary measurements. We use an asymptotic characterization of the effect of small shape changes on boundary measurements to get an explicit form of the map from the shape perturbations to the boundary data. In section 3 we describe different strategies for solving the reconstruction problem from limited-view data. Section 4 is devoted to the regime where the interface of the conductivity inclusion is located just below the boundary of the background domain. We provide an inverse filtering approach to estimate the shape perturbations and prove that we can resolve for any fixed SNR a sufficiently shallow shape perturbation on the overlap of the source and receiver apertures. In section 5 we consider the case where the inclusion is small and perform a matrix filtering approach to get the lowest modes of the shape perturbation in this case. It is worth mentioning that a filtering approach with a diagonal scaling would not work in this case because of a mode coupling. A reasonable inverse filter should include off-diagonal terms in this case and therefore should be a matrix one. The paper ends with a short discussion.

2. Interface Estimation with Limited-View Data

In this section we formulate the reconstruction problem in the case of limited-view noisy conductivity data in the two-dimensional case. We contrast this process with estimation based on full-view measurements and find the connection between the full- and the limited-view cases. For simplicity, we consider inclusions with constant conductivities and image only small changes in their shapes.

2.1. **Differential Measurements.**

The partial measurements are taken on a circle of unit radius in our non-dimensionalized setting. The domain of interest,

encapsulated by the measurements, is thus

$$\Omega = \left\{ \boldsymbol{x} = r\boldsymbol{e}_\theta \mid r \leq 1,\, -\pi \leq \theta < \pi \right\}, \tag{1}$$

where $\boldsymbol{e}_\theta = (\cos\theta, \sin\theta)$. Imbedded in the domain there is a homogeneous inclusion centered at the origin and with the shape of a perturbed circle. Our objective is to estimate the rim of the inclusion. We denote the domain of the unperturbed disk by D and the perturbed domain by D_ε:

$$D = \left\{ \boldsymbol{x} = r\boldsymbol{e}_\theta \mid r \leq \alpha,\, -\pi \leq \theta < \pi \right\}, \tag{2}$$

$$D_\varepsilon = \left\{ \boldsymbol{x} = r\boldsymbol{e}_\theta \mid r \leq \alpha + \varepsilon h(\theta),\, -\pi \leq \theta < \pi \right\}. \tag{3}$$

We let here h to be of order one and assume that h is of class $\mathcal{C}^1$ and $\varepsilon \ll 1$.

A central point of our analysis will be to consider partial aperture. We refer to [6] for the full aperture case. The source aperture is parameterized by $(\cos(\theta), \sin(\theta)); \theta \in (-\phi_s, \phi_s)$ and the receiver aperture is parameterized by $(\cos(\theta), \sin(\theta)); \theta \in (\phi_c - \phi_r, \phi_c + \phi_r)$.

For analysis of the case with partial measurements it will be convenient with a notation for the aperture or source function:

$$\psi_m^\phi(\theta) \equiv \begin{cases} e^{-im\theta\pi/\phi}, & |\theta| < \phi \\ 0, & \text{else.} \end{cases}$$

Given $0 < \phi_s < \pi$, the field for different source configurations are indexed by $m = 0, \pm 1, \pm 2, \ldots$ and chosen to solve in the perturbed case:

$$\nabla \cdot (1 + (k-1)\chi_{D_\varepsilon}) \nabla u_\varepsilon^m(\boldsymbol{x}) = 0\,, \qquad \boldsymbol{x} \in \Omega\,,$$

with the Neumann boundary conditions at the surface $\partial\Omega$:

$$\frac{\partial u_\varepsilon^m}{\partial \nu}(\boldsymbol{e}_\theta) = \psi_m^{\phi_s}(\theta)\,, \qquad \theta \in [-\pi, \pi)\,, \qquad\qquad \int_{-\pi}^{\pi} u_\varepsilon^m(\boldsymbol{e}_\theta) d\theta = 0\,.$$

Here, χ_{D_ε} is the characteristic function of D_ε, ν denotes the outward normal to $\partial\Omega$ and the positive constant k is the contrast in the conductivity between the inclusion and the background.

The field corresponding to the *unperturbed* domain D is denoted by $u^m = u_0^m$. The *differential* measurements are now denoted by

$$\hat{a}_{n,m} = \int_{\phi_c - \phi_r}^{\phi_c + \phi_r} e^{-in(\theta - \phi_c)\pi/\phi_r} (u_\varepsilon^m - u^m)(\boldsymbol{e}_\theta) d\theta\,.$$

We use the Fourier convention

$$\hat{h}_p = \int_{-\pi}^{\pi} h(\theta) \frac{e^{-ip\theta}}{2\pi} d\theta\,, \qquad h(\theta) = \sum_{p=-\infty}^{\infty} \hat{h}_p e^{ip\theta}\,,$$

and

$$\check{\psi}(p) = \int_{-\pi}^{\pi} \psi(\theta) \frac{e^{ip\theta}}{2\pi} d\theta\,, \qquad \psi(\theta) = \sum_{p=-\infty}^{\infty} \check{\psi}(p) e^{-ip\theta}\,.$$

For the full measurements corresponding to the "full aperture sources" we use the notation

$$u^{m,\pi}(\theta, r) = u^m(\theta, r) \mid_{\phi_s = \pi}\,, \qquad u_\varepsilon^{m,\pi}(\theta, r) = u_\varepsilon^m(\theta, r) \mid_{\phi_s = \pi}\,. \tag{4}$$

The following lemma clarifies the relations between the differential measurements with partial aperture and the differential measurements with full aperture.

Lemma 2.1. *The differential measurements $\hat{a}_{n,m}$ corresponding to a source aperture ϕ_s and a receiver aperture ϕ_r can be expressed in terms of those corresponding to the full-view case ($\phi_s = \phi_r = \pi$), $\hat{a}^{\pi}_{n,m}$, as follows*

$$\hat{a}_{n,m} = \sum_{\tilde{p},p=-\infty}^{\infty} \check{\psi}^{\phi_r}_n(\tilde{p})\check{\psi}^{\phi_s}_m(p)e^{i\tilde{p}\phi_c}\hat{a}^{\pi}_{\tilde{p},p}\,,$$

where the filters $\check{\psi}^{\phi_r}_n$ and $\check{\psi}^{\phi_s}_m$ are defined by

$$\check{\psi}^{\phi}_m(p) = \frac{\phi}{\pi}\mathrm{sinc}(m\pi - p\phi)\,, \tag{5}$$

and

$$\hat{a}^{\pi}_{\tilde{p},p} = \int_{-\pi}^{\pi}(u^{p,\pi}_{\varepsilon} - u^{p,\pi})(\boldsymbol{e}_\theta)e^{-i\tilde{p}\theta}d\theta\,.$$

Proof. From (4) we have

$$u^m(\theta,r) = \sum_{p=-\infty}^{\infty}\check{\psi}^{\phi_s}_m(p)u^{p,\pi}(\theta,r)\,, \qquad u^m_{\varepsilon}(\theta,r) = \sum_{p=-\infty}^{\infty}\check{\psi}^{\phi_s}_m(p)u^{p,\pi}_{\varepsilon}(\theta,r)\,,$$

where $\check{\psi}^{\phi_r}_n$ and $\check{\psi}^{\phi_s}_m$ are defined by (5). Note that $\check{\psi}^{\phi}_0(0) = \phi/\pi$ and $\check{\psi}^{\phi}_m(0) = 0$ for $m \neq 0$. With this parameterization we have the following representation of the measurements (in the absence of measurement noise):

$$\begin{aligned}\hat{a}_{n,m} &\equiv \int_{-\pi}^{\pi}\psi^{\phi_r}_n(\theta-\phi_c)\sum_{p=-\infty}^{\infty}\check{\psi}^{\phi_s}_m(p)(u^{p,\pi}_{\varepsilon} - u^{p,\pi})(\boldsymbol{e}_\theta)d\theta \\ &= \int_{-\pi}^{\pi}\sum_{\tilde{p}=-\infty}^{\infty}\check{\psi}^{\phi_r}_n(\tilde{p})e^{-i\tilde{p}\theta}e^{i\tilde{p}\phi_c}\sum_{p=-\infty}^{\infty}\check{\psi}^{\phi_s}_m(p)(u^{p,\pi}_{\varepsilon} - u^{p,\pi})(\boldsymbol{e}_\theta)d\theta\,,\end{aligned}$$

which completes the proof of the lemma. □

In our analysis we moreover make use of asymptotic characterization of the differential measurements to get explicit results on the resolving power of the measurements. This representation uses the results of [8]. We have, for any $|n|, |m| \ll (1/\epsilon)$, the representation

$$\hat{a}^{\pi}_{n,m} = \varepsilon c_{n,m}(\alpha,k)\hat{h}_{n+m} + \varepsilon^2\hat{V}^{\pi}_{n,m}\,,$$

with the coefficients

$$c_{n,m}(\alpha,k) = -\frac{8\pi(k-\mathrm{sign}(nm))}{\alpha(k-1)}\frac{1}{(\alpha^{-|n|\frac{k+1}{k-1}} + \alpha^{|n|})(\alpha^{-|m|\frac{k+1}{k-1}} + \alpha^{|m|})}\,, \tag{6}$$

if $nm \neq 0$, and $c_{n,m}(\alpha,k) = 0$ if $nm = 0$. Here, $\varepsilon^2\hat{V}^{\pi}_{n,m}$ is the approximation error (more exactly, the linearization error) for the full aperture case, of order ε^2 when $\varepsilon \ll 1$.

The linearization of the map from the perimeter perturbation $(\hat{h}_p)_{p=-\infty}^{+\infty}$ to the data $(\hat{a}_{n,m})_{n,m=-\infty}^{+\infty}$ is described by the linear operator $\mathcal{Q}$ defined by

$$(\mathcal{Q}\hat{h})_{n,m} := \varepsilon\sum_{\tilde{p},p=-\infty}^{\infty}\check{\psi}^{\phi_r}_n(\tilde{p})\check{\psi}^{\phi_s}_m(p)e^{i\tilde{p}\phi_c}c_{\tilde{p},p}(\alpha,k)\hat{h}_{\tilde{p}+p}\,. \tag{7}$$

Our objective is to assess the resolving power of limited-view data in the presence of measurement or instrument noise. The measured data can be expressed as

$$\hat{a}^{\rm meas}_{n,m} = (\mathcal{Q}\hat{h})_{n,m} + \sigma \hat{W}_{n,m} + \varepsilon^2 \hat{V}_{n,m}\,, \tag{8}$$

with the noise terms $\hat{W}_{n,m}$ modeled as independent standard complex circularly symmetric Gaussian random variables (such that $\mathbb{E}[|\hat{W}_{m,n}|^2] = 1$; $\mathbb{E}$ being the expectation) and σ modeling the noise magnitude. The term $\varepsilon^2\hat{V}_{n,m}$ models the linearization error and we shall focus on the case $\varepsilon^2 \ll \sigma$ so that the measurement error is the dominant error. We therefore focus on this contribution to the error and write with some abuse of notation:

$$\hat{a}^{\rm meas}_{n,m} = (\mathcal{Q}\hat{h})_{n,m} + \sigma \hat{W}_{n,m}\,. \tag{9}$$

2.2. **The Linear Operator.** Our objective is now to identify the rim or perimeter perturbation of the inclusion, that is the function h. As shown in [6], only $\hat{h}_p$ for $0 < |p| \ll 1/\varepsilon$ can be reconstructed from boundary measurements in the linearized context, otherwise the linearization error $\varepsilon^2\hat{V}_{n,m}$ is too large. Therefore, let $M \ll 1/\varepsilon$ be a positive integer and suppose that $\hat{h}_p = 0$ for $|p| \geq M$.

We start by noting that the adjoint of the operator $\mathcal{Q}$ is

$$(\mathcal{Q}^\star \hat{a})_p = \varepsilon \sum_{j,m,n=-\infty}^{\infty} \check{\psi}^{\phi_r}_n(p-j)\check{\psi}^{\phi_s}_m(j) e^{i(j-p)\phi_c} c_{p-j,j}(\alpha,k)\,\hat{a}_{n,m}\,. \tag{10}$$

We moreover have

$$\begin{aligned}(\mathcal{Q}^\star\mathcal{Q}\hat{h})_p &= \varepsilon^2 \sum_{j,m,n=-\infty}^{\infty} e^{i(n+j-p)\phi_c}\mathcal{H}^{\phi_r}(p-j-n)\mathcal{H}^{\phi_s}(j-m)\\ &\qquad \times c_{p-j,j}(\alpha,k)c_{n,m}(\alpha,k)\hat{h}_{n+m}\,,\end{aligned}$$

where we have introduced

$$\mathcal{H}^\phi(p) = \sum_{n=-\infty}^{\infty} \check{\psi}^\phi_n(\tilde{p})\check{\psi}^\phi_n(\tilde{p}+p) = \frac{\phi^2}{\pi^2}{\rm sinc}(\phi p)\,. \tag{11}$$

In order to simplify somewhat the expressions involved in the reconstruction of h we shall assume from now a relatively high contrast situation with $k \gg 1$ and make the replacement:

$$c_{n,m}(\alpha,k) = c_{n,m}(\alpha), \qquad c_{n,m}(\alpha) := \frac{-8\pi}{\alpha\left(\alpha^{|n|}+\alpha^{-|n|}\right)\left(\alpha^{|m|}+\alpha^{-|m|}\right)}\,, \tag{12}$$

so that we have

$$\begin{aligned}(\mathcal{Q}^\star\mathcal{Q}\hat{h})_p &= \varepsilon^2\frac{\phi_s^2\phi_r^2}{\pi^4}\sum_{j,m,n=-\infty}^{\infty} e^{i(n+j-p)\phi_c}{\rm sinc}(\phi_r(p-j-n))\\ &\qquad \times{\rm sinc}(\phi_s(j-m))c_{p-j,j}(\alpha)c_{n,m}(\alpha)\hat{h}_{n+m}\,.\end{aligned} \tag{13}$$

2.3. **The Full Aperture Case.** We review here briefly the full aperture case with $\phi_s = \phi_r = \pi$ that was treated in detail in [6]. We have

$$(\mathcal{Q}^\star \mathcal{Q}\hat{h})_p = \varepsilon^2 q_p(\alpha)\hat{h}_p\,, \qquad q_p(\alpha) = \sum_{j=-\infty}^{\infty} c_{p-j,j}(\alpha)^2\,. \tag{14}$$

Compared to (13), note the diagonal character of $\mathcal{Q}^\star\mathcal{Q}$ in the full-view case. The least squares estimate of $\hat{h}_p$ using $\hat{a}^{\rm meas}$ is

$$\begin{aligned} \hat{h}_p^{\rm est} &= \big((\mathcal{Q}^*\mathcal{Q})^{-1}\mathcal{Q}^*\hat{a}^{\rm meas}\big)_p = \varepsilon^{-2} q_p(\alpha)^{-1}\,(\mathcal{Q}^*\hat{a}^{\rm meas})_p \\ &= \hat{h}_p + \sigma\varepsilon^{-2} q_p(\alpha)^{-1}(\mathcal{Q}^*\hat{W})_p\,. \end{aligned} \tag{15}$$

Using

$$\mathbb{E}[\overline{\hat{W}_{n,m}}\hat{W}_{n',m'}] = \mathbf{1}_n(n')\mathbf{1}_m(m'),$$

where $\mathbf{1}_n(n') = 1$ if $n = n'$ and 0 otherwise, we find

$$\mathbb{E}\big[\big|(\mathcal{Q}^*\hat{W})_p\big|^2\big] = (\mathcal{Q}^*\mathcal{Q}\mathbf{1}_p)_p\,, \tag{16}$$

which gives using (14):

$$\mathbb{E}\big[\big|(\mathcal{Q}^*\hat{W})_p\big|^2\big] = \varepsilon^2 q_p(\alpha)\,,$$

and we then have

$$\mathbb{E}\Big[\big|\hat{h}_p^{\rm est} - \hat{h}_p\big|^2\Big] = q_p(\alpha)^{-1}\frac{\sigma^2}{\varepsilon^2}\,. \tag{17}$$

We can therefore conclude from (17) that in order to resolve the pth mode of h, $\hat{h}_p$, we need the following resolving condition to be satisfied:

$$\frac{\sigma^2}{\varepsilon^2} < q_p(\alpha)\,.$$

We introduce the signal-to-noise ratio SNR:

$$\mathrm{SNR} = \frac{\varepsilon^2}{\sigma^2}\,. \tag{18}$$

Using (12) we find that a mode resolving sufficient condition when $\alpha \ll 1$ is

$$\mathrm{SNR}^{-1} < \begin{cases} 32\pi^2\alpha^{2|p|-2}(2|p|-1) & \text{if } |p| \geq 1, \\ 4\pi^2\alpha^{-2} & \text{if } p = 0. \end{cases} \tag{19}$$

Using (12) and

$$\sum_{y=-\infty}^{\infty} \frac{1}{(\alpha^{|y|} + \alpha^{-|y|})^4} \overset{\alpha\to 1}{\simeq} \frac{2}{1-\alpha}\int_0^\infty \frac{dx}{(e^x + e^{-x})^4} = \frac{1}{12(1-\alpha)}\,, \tag{20}$$

we find a mode resolving sufficient condition when $\alpha \to 1$ is

$$\mathrm{SNR}^{-1} < \frac{16\pi^2}{3(1-\alpha)}\,. \tag{21}$$

We can see in particular that we have "infinite resolution" in the limit $\alpha \to 1$ in the sense that we can estimate all modes $\hat{h}_p$ in this limit.

When $\alpha \ll 1$ we can estimate the modes $\hat{h}_p$ with $|p| \le p_{\max}$ where

$$p_{\max} = \begin{cases} -\infty & \text{if SNR} < \dfrac{\alpha^2}{4\pi^2}, \\ 0 & \text{if } \dfrac{\alpha^2}{4\pi^2} < \text{SNR} < \dfrac{1}{32\pi^2}, \\ p & \text{if } \dfrac{\alpha^2}{2p-1}\dfrac{\alpha^{-2p}}{32\pi^2} < \text{SNR} < \dfrac{1}{2p+1}\dfrac{\alpha^{-2p}}{32\pi^2}, \quad p \ge 1\,. \end{cases} \tag{22}$$

3. Strategies in The Partial Aperture Case

In this section we outline different approaches for solving the reconstruction problem with limited-view data.

Using (12) and (13) we have the following lemma.

Lemma 3.1. *We have*

$$(\mathcal{Q}^\star \mathcal{Q}\hat{h})_p = \varepsilon^2 \sum_{x=-\infty}^{\infty} H_{p,x}(\alpha)\hat{h}_x\,, \tag{23}$$

where

$$H_{p,x}(\alpha) = \frac{\phi_s^2\phi_r^2}{\pi^4} \sum_{y,z=-\infty}^{\infty} e^{-iz\phi_c}\mathrm{sinc}(\phi_r z)\mathrm{sinc}(\phi_s(p-x-z)) \times c_{p-y,y}(\alpha)c_{p-(y+z),(y+z)-p+x}(\alpha)\,. \tag{24}$$

As mentioned above, in the full aperture case $\phi_r = \phi_s = \pi$ the matrix $H(\alpha)$ becomes diagonal:

$$H_{p,x}(\alpha) = q_p(\alpha)\mathbf{1}_p(x)\,,$$

where $\mathbf{1}_p(x) = 1$ if $x = p$ and 0 otherwise, and we can obtain an estimate of the perimeter perturbations h by a simple diagonal scaling (see Subsection 2.3). In the limited-view case this matrix is complicated and we need to construct an approximate inverse.

One approach to constructing such an inverse would be to use the Singular Value Decomposition of $H_{p,x}(\alpha)$ and construct a regularized or pseudo inverse, the cutoff or regularization is then chosen according to the noise magnitude. However, in this case the explicit form of the Singular Value Decomposition is not known.

A second approach would be to minimize over h the discrepancy functional

$$\frac{1}{2}\sum_{p=-\infty}^{\infty}\left|\sum_{x=-\infty}^{\infty} H_{p,x}(\alpha)\hat{h}_x - (\mathcal{Q}^\star \hat{a}^{\text{mes}})_p\right|^2 + \eta\Big(\sum_{p=-\infty}^{\infty}|\hat{h}_p|^r\Big)^{1/r}, \tag{25}$$

where $\hat{a}^{\text{mes}} = (\hat{a}^{\text{meas}}_{n,m})_{n,m=-\infty}^{+\infty}$, η is a regularization parameter, and r is a positive real. Choosing $r = 1$ promotes sparse minimal solutions [14]. The algorithm of Beck and Teboulle [11] can be used in this case to efficiently compute the minimizer.

A third simpler and direct approach would be inverse filtering [21]. We can use a diagonal scaling and construct an estimate as

$$\hat{h}^{\text{est}}_p = \varepsilon^{-2} A_p(\alpha)(\mathcal{Q}^\star \hat{a}^{\text{mes}})_p\,. \tag{26}$$

We will see that this strategy gives good results when α is close to one or when the source and receiver apertures are full, but it fails when the source or receiver aperture is partial and the inclusion is small, because any reasonable inverse must

include off-diagonal terms in this case. Therefore, the strategy when α is small is to look for a matrix (filter) B such that

$$\hat{h}_p^{\rm est} = \varepsilon^{-2} \sum_{r=-\infty}^{\infty} B_{p,r}(\alpha)(\mathcal{Q}^\star \hat{a}^{\rm mes})_r \,. \tag{27}$$

A good candidate for $B(\alpha)$ is of course the (pseudo-)inverse of the matrix $H(\alpha)$, in the sense that it is the least-square solution. This is the basis of our strategy, and we will show how to construct this pseudo-inverse in an efficient and stable way.

4. Estimation of the Perimeter Perturbation for a Large Radius Ball

In this section we consider the regime where the interface of the conductivity inclusion is located just below the boundary of the background domain. We show that an inverse filtering approach with a diagonal scaling allows us to estimate the shape perturbations. Moreover, we prove that one can resolve for any fixed SNR a sufficiently shallow shape perturbation on the overlap of the source and receiver apertures.

We consider the approach (26). Following the inverse filtering approach (26), the estimator

$$h^{\rm est}(\theta) = \varepsilon^{-2} \sum_{p=-\infty}^{\infty} A_p(\alpha)(\mathcal{Q}^\star \hat{a}^{\rm mes})_p e^{ip\theta} \,, \tag{28}$$

has mean

$$\begin{aligned} \mathbb{E}[h^{\rm est}(\theta)] = \frac{\phi_s^2 \phi_r^2}{\pi^4} \sum_{p,x,y,z=-\infty}^{\infty} & A_p(\alpha) e^{-iz\phi_c} {\rm sinc}(\phi_r z) {\rm sinc}(\phi_s x) \\ & \times c_{p-y,y}(\alpha) c_{p-y-z,y-x}(\alpha) \hat{h}_{p-x-z} e^{ip\theta} \,. \end{aligned} \tag{29}$$

The fluctuations due to measurement error are

$$\begin{aligned} e^{\rm est}(\theta) &= h^{\rm est}(\theta) - \mathbb{E}[h^{\rm est}(\theta)] \\ &= \frac{\sigma}{\varepsilon^2} \sum_{p=-\infty}^{\infty} A_p(\alpha)(\mathcal{Q}^\star \hat{W})_p e^{ip\theta} \\ &= \frac{\sigma}{\varepsilon} \frac{\phi_s \phi_r}{\pi^2} \sum_{j,n,m,p=-\infty}^{\infty} A_p(\alpha) {\rm sinc}(n\pi - (p-j)\phi_r) {\rm sinc}(m\pi - j\phi_s) \\ &\quad \times e^{i(j-p)\phi_c} c_{p-j,j}(\alpha) \hat{W}_{n,m} e^{ip\theta} \,. \end{aligned} \tag{30}$$

In this section we consider the regime when the interface is located just below the surface $\alpha \to 1$. We will prove that we can resolve for any fixed SNR a sufficiently shallow perimeter perturbation of a conductivity inclusion on the overlap of the source and receiver apertures.

It turns out that the operator $\mathcal{Q}^\star \mathcal{Q}$ is (approximately) diagonal on the overlap of the source and receiver arrays. The following result holds.

Lemma 4.1. *When $\alpha \to 1$, we have*

$$\sum_{p=-\infty}^{\infty} (\mathcal{Q}^\star \mathcal{Q} \hat{h})_p e^{ip\theta} = \varepsilon^2 \phi_r \phi_s \frac{8}{1-\alpha} \begin{cases} h(\theta) + O(1-\alpha) & \text{if } \theta \in \chi_{\phi_r,\phi_s,\phi_c}, \\ O(1-\alpha) & \text{otherwise,} \end{cases}$$

where $\chi_{\phi_r,\phi_s,\phi_c}$ *is the overlap of the source aperture and the receiver aperture:*

$$\chi_{\phi_r,\phi_s,\phi_c} = \{\theta \in [-\pi,\pi] \mid \theta \in [-\phi_s,\phi_s] \,\text{modulo}\, 2\pi \text{ and } \theta \in [\phi_c-\phi_r,\phi_c+\phi_r] \,\text{modulo}\, 2\pi\}\,.$$

Proof. We consider (23-24) and replace the sinc functions by $\text{sinc}(s/2) = \int_{-1/2}^{1/2} e^{isu} du$. We get via the change of variables $n = p-(y+z); m = (y+z)-p+x$:

$$\sum_{p=-\infty}^{\infty} (\mathcal{Q}^\star\mathcal{Q}\hat{h})_p e^{ip\theta} = \frac{\varepsilon^2\phi_r^2\phi_s^2}{\pi^4} \sum_{m,n=-\infty}^{\infty} \int_{-1/2}^{1/2} du \int_{-1/2}^{1/2} du' \sum_{p=-\infty}^{\infty} e^{ip(-\phi_c+2\phi_r u+\theta)}$$
$$\times \sum_{y=-\infty}^{\infty} e^{iy(\phi_c-2\phi_r u+2\phi_s u')} e^{in(\phi_c-2\phi_r u)} e^{-2im\phi_s u'} c_{n,m}(\alpha) c_{p-y,y}(\alpha) \hat{h}_{n+m}\,.$$

When $\alpha \to 1$ we can replace $c_{p-y,y}(\alpha)$ by -2π up to a factor $(1-\alpha)$ and we make use of the Poisson summation formula $\sum_p e^{ip\theta} = 2\pi \sum_k \delta(\theta - k2\pi)$ to arrive at

$$\sum_{p=-\infty}^{\infty} (\mathcal{Q}^\star\mathcal{Q}\hat{h})_p e^{ip\theta} = -\frac{2\varepsilon^2\phi_r\phi_s}{\pi} \mathbf{1}_{\chi_{\phi_r,\phi_s,\phi_c}}(\theta)$$
$$\times \sum_{m,n=-\infty}^{\infty} e^{i(n+m)\theta} c_{n,m}(\alpha) \hat{h}_{n+m} \Big(1 + O(1-\alpha)\Big)\,.$$

By substituting the expression (12) for $c_{n,m}(\alpha)$ and by using that

$$\sum_{y=-\infty}^{\infty} \frac{1}{(\alpha^{|y|}+\alpha^{-|y|})^2} \overset{\alpha\to 1}{\simeq} \frac{2}{1-\alpha} \int_0^\infty \frac{dx}{(e^x+e^{-x})^2} = \frac{1}{2(1-\alpha)}\,,$$

we get the desired result. □

The previous lemma gives the form of the inverse filter that we should use. The following proposition holds.

Proposition 4.2. *If we choose*

$$A_p(\alpha) = \frac{1-\alpha}{8\phi_r\phi_s}\,,$$

then the estimator (28) satisfies in the regime $\alpha \to 1$

$$h^{\text{est}}(\theta) = \begin{cases} h(\theta) + O(1-\alpha) & \text{if } \theta \in \chi_{\phi_r,\phi_s,\phi_c}\,, \\ O(1-\alpha) & \text{otherwise.} \end{cases}$$

Furthermore, we obtain for fixed SNR *defined by (18) that*

$$\mathbb{E}[|\hat{e}_p^{\text{est}}|^2] = \text{SNR}^{-1} \frac{|\chi_{\phi_r,\phi_s,\phi_c}|(1-\alpha)}{24\pi\phi_r\phi_s} \Big(1 + O(1-\alpha)\Big) \overset{\alpha\to 1}{\longrightarrow} 0\,,$$

where $|\chi_{\phi_r,\phi_s,\phi_c}|$ *is the angular length of the overlap of the source aperture and the receiver aperture.*

Proof. We have in the regime $\alpha \to 1$ using (11) and (30):

$$\begin{aligned}\mathbb{E}[|\hat{e}_p^{\rm est}|^2] &= \frac{\sigma^2}{\varepsilon^2} A_p(\alpha)^2 \sum_{j,l,m,n=-\infty}^{\infty} \check{\psi}_n^{\phi_r}(p-j)\check{\psi}_m^{\phi_s}(j) e^{i(j-p)\phi_c} c_{p-j,j}(\alpha) \\ &\quad \times \check{\psi}_n^{\phi_r}(p-l)\check{\psi}_m^{\phi_s}(l) e^{-i(l-p)\phi_c} c_{p-l,l}(\alpha) \\ &= \frac{\sigma^2}{\varepsilon^2}\frac{\phi_r^2\phi_s^2}{\pi^4}\Big(\sum_{z=-\infty}^{\infty} e^{-iz\phi_c}{\rm sinc}(z\phi_r){\rm sinc}(z\phi_s)\Big) A_p(\alpha)^2 \\ &\quad \times \Big(\sum_{y=-\infty}^{\infty} \frac{64\pi^2}{(\alpha^{|y|}+\alpha^{-|y|})^4}\Big)\Big(1+O(1-\alpha)\Big)\,.\end{aligned}$$

Using (20) and computing the sum over z:

$$\sum_{z=-\infty}^{\infty} e^{-iz\phi_c}{\rm sinc}(z\phi_r){\rm sinc}(z\phi_s) = \frac{\pi|\chi_{\phi_r,\phi_s,\phi_c}|}{2\phi_r\phi_s}\,,$$

we get the desired result. □

Proposition 4.2 shows that a sufficiently shallow perimeter perturbation on the aperture overlap can be resolved for any SNR.

5. Estimation of the Perimeter Perturbation for a Small Radius Ball

In this section we consider the case where the inclusion is of small radius. Because of the mode coupling in this case, we perform a matrix filtering approach to get the lowest modes of the shape perturbation in this case.

5.1. The Case of Full Receiver and Partial Source Apertures.

In this subsection we consider the case when the receiver aperture is full so that $\phi_r = \pi$. The case of partial receiver and full source apertures can be treated in exactly the same manner.

In the absence of measurement noise, we have $\hat{a}^{\rm mes} = \mathcal{Q}\hat{h}$ and

$$(\mathcal{Q}^\star \hat{a}^{\rm mes})_p = \frac{\varepsilon^2\phi_s^2}{\pi^2}\sum_{x=-\infty}^{\infty} {\rm sinc}(\phi_s x) X_{p,x}(\alpha)\hat{h}_{p-x}\,, \tag{31}$$

where

$$X_{p,x}(\alpha) = \sum_{y=-\infty}^{\infty} c_{p-y,y}(\alpha)c_{p-y,y-x}(\alpha)\,.$$

If we consider that (31) is an estimate $\hat{h}_p^{\rm est}$ of $\hat{h}_p$, then we can write that its inverse Fourier transform is an estimate of $h(\theta)$ that has the form

$$\begin{aligned} h^{\rm est}(\theta) &= \sum_{p=-\infty}^{\infty} (\mathcal{Q}^\star \hat{a}^{\rm mes})_p e^{ip\phi} \\ &= \frac{\varepsilon^2\phi_s^2}{\pi^2}\int_{-\pi}^{\pi} \mathcal{K}(\theta,\theta')h(\theta')d\theta'\,, \end{aligned} \tag{32}$$

where the imaging kernel (parameterized by ϕ_s and α) is given by

$$\mathcal{K}(\theta,\theta') = \frac{1}{4\pi\phi_s}\int_{-\phi_s}^{\phi_s} \check{X}(\theta-\theta', v+\theta';\alpha)dv\,, \tag{33}$$

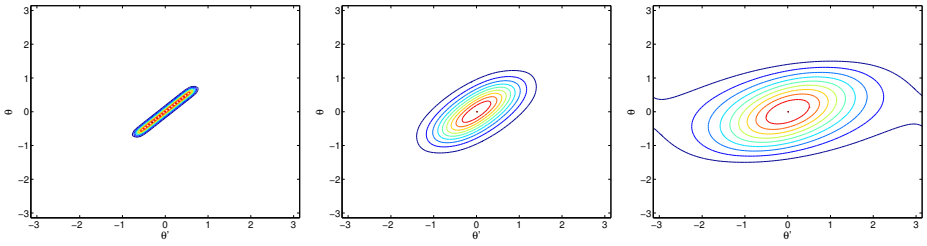

FIGURE 1. Level curves of the imaging kernel $\mathcal{K}(\theta, \theta')$ for $\phi_s = \pi/5$ and for $\alpha = 0.9$ (left), $\alpha = 0.5$ (center), and $\alpha = 0.2$ (right).

for

$$\check{X}(\theta, \theta'; \alpha) = \sum_{p,x=-\infty}^{\infty} X_{p,x}(\alpha) e^{i(p\theta + x\theta')} .$$

Note that an ideal case with perfect estimation would mean that the imaging kernel is proportional to $\mathcal{K}(\theta, \theta') = \delta(\theta - \theta')$.

In Figure 1 we plot (up to a normalization constant) the imaging kernel $\mathcal{K}(\theta, \theta')$ for $\phi_s = \pi/5$ and for $\alpha = 0.9, 0.5, 0.2$. One can observe that, when α is close to one, the kernel is close to $\mathbf{1}_{[-\phi_s, \phi_s]}(\theta)\delta(\theta - \theta')$, which means that the perturbation $h(\theta)$ can be estimated with accuracy over the source aperture, as predicted by Proposition 4.2. One can also observe that, when α is much smaller than one, the imaging kernel becomes bad, which is related to the fact that the information provided by the measurements is reduced. Figure 2 illustrates this by plotting the singular value spectrum of the Fourier transform $\hat{\mathcal{K}}_{p,p'}$ of the imaging kernel for $\alpha = 0.9, 0.5, 0.2$, up to a common normalization factor. Note that the first singular values increase for very small radii α, corresponding to enhanced resolvability for the first modes for very small radii. In Figure 3 we show the first left singular vector of the Fourier transform $\hat{\mathcal{K}}_{p,p'}$ of the imaging kernel for $\phi_s = \pi/5$ and for $\alpha = 0.9, 0.5, 0.2$. Note that for small radii information from only the leading modes can be associated with the first singular vector while for larger radii the first singular vector depends on a combination of modes.

It is thus clear that in the regime of small radii α only the lowest modes can be resolved, even with small amounts of noise, and that the estimation should involve a matrix filter B as in (27). Thus, to get a measure of resolution noise needs to be taken into account. We next carry out such an analysis that discusses these issues in detail and also the form of the matrix filter for the lowest modes in the situation with a small inclusion.

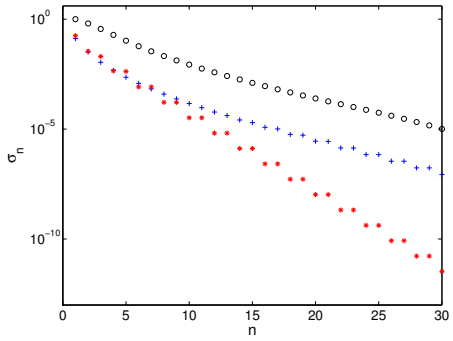

FIGURE 2. The singular values of the Fourier transform $(\hat{\mathcal{K}}_{p,p'})_{p,p'=-\infty}^{\infty}$ of the imaging kernel for $\phi_s = \pi/5$ and for $\alpha = 0.9$ (circles), $\alpha = 0.5$ (crosses), and $\alpha = 0.2$ (stars).

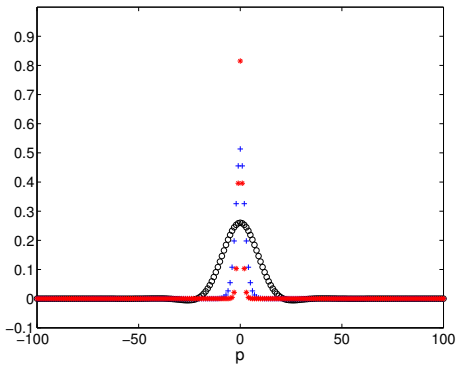

FIGURE 3. The first left singular vectors of the Fourier transform $(\hat{\mathcal{K}}_{p,p'})_{p,p'=-\infty}^{\infty}$ of the imaging kernel for $\phi_s = \pi/5$ and for $\alpha = 0.9$ (circles), $\alpha = 0.5$ (crosses), and $\alpha = 0.2$ (stars). We plot the moduli of the coefficients of the vectors.

When $\alpha \ll 1$, we can expand $X_{p,x}(\alpha)$ in terms of α and find

$$\begin{aligned}(\mathcal{Q}^\star \hat{a}^{\rm mes})_0 &= \frac{64\varepsilon^2\phi_s^2}{\alpha^2}\Big[\frac{1}{16}\hat{h}_0 + \frac{\alpha}{8}\mathrm{sinc}(\phi_s)(\hat{h}_1+\hat{h}_{-1}) \\ &\quad + \frac{\alpha^2}{8}\mathrm{sinc}(2\phi_s)(\hat{h}_2+\hat{h}_{-2}) + O(\alpha^3)\Big], \end{aligned} \tag{34}$$

$$\begin{aligned}(\mathcal{Q}^\star \hat{a}^{\rm mes})_1 &= \frac{64\varepsilon^2\phi_s^2}{\alpha^2}\Big[\frac{\alpha^2}{2}\hat{h}_1 + \frac{\alpha}{8}\mathrm{sinc}(\phi_s)\hat{h}_0 \\ &\quad + \frac{\alpha^2}{4}\mathrm{sinc}(2\phi_s)\hat{h}_{-1} + O(\alpha^3)\Big], \end{aligned} \tag{35}$$

and

$$(\mathcal{Q}^\star \hat{a}^{\rm mes})_{-1} = \overline{(\mathcal{Q}^\star \hat{a}^{\rm mes})_1}, \quad (\mathcal{Q}^\star \hat{a}^{\rm mes})_p = O(\alpha^{p-2}) \qquad \text{for all } p \geq 2.$$

It is important to note the presence of the term $\frac{\alpha}{8}\mathrm{sinc}(\phi_s)\hat{h}_0$ in $(\mathcal{Q}^\star \hat{a}^{\mathrm{mes}})_1$, which is much larger (when $\phi_s < \pi$) than $\frac{\alpha^2}{2}\hat{h}_1$. As a consequence, $\hat{h}_1$ cannot be estimated by looking at $(\mathcal{Q}^\star \hat{a}^{\mathrm{mes}})_{\pm 1}$ only. It is therefore critical to use an inverse filter with off-diagonal terms.

In order to estimate $\hat{h}_0$, we first propose to look for an estimator of the form

$$\hat{h}_0^{\mathrm{est},(1)} = \varepsilon^{-2} B_{0,0}^{(1)}(\alpha)(\mathcal{Q}^\star \hat{a}^{\mathrm{mes}})_0\,, \tag{36}$$

and to identify the best coefficient $B_{0,0}^{(1)}$ (in the least square sense). From (34) we find that

$$B_{0,0}^{(1)} = \frac{\alpha^2}{4\phi_s^2}\,,$$

which yields

$$\hat{h}_0^{\mathrm{est},(1)} = \hat{h}_0 + O(\alpha)\,. \tag{37}$$

In order to estimate $\hat{h}_p$, $p = 0, 1$, we may look for estimators of the form

$$\hat{h}_p^{\mathrm{est},(2)} = \varepsilon^{-2} \sum_{l=-1}^{1} B_{p,l}^{(2)}(\alpha)(\mathcal{Q}^\star \hat{a}^{\mathrm{mes}})_l, \tag{38}$$

and identify the best coefficients $(B_{p,l}^{(2)})_{p=0,1,l=-1,0,1}$ (in the least square sense). From (35) we get

$$\begin{aligned}
B_{0,0}^{(2)} &= \frac{\alpha^2}{64\phi_s^2}\frac{16(2+\mathrm{sinc}(2\phi_s))}{2-2\mathrm{sinc}^2(\phi_s)+\mathrm{sinc}(2\phi_s)}\,,\\
B_{0,-1}^{(2)} &= -\frac{\alpha^2}{64\phi_s^2}\frac{1}{\alpha}\frac{8\mathrm{sinc}(\phi_s)}{2-2\mathrm{sinc}^2(\phi_s)+\mathrm{sinc}(2\phi_s)}\,,\\
B_{0,1}^{(2)} &= -\frac{\alpha^2}{64\phi_s^2}\frac{1}{\alpha}\frac{8\mathrm{sinc}(\phi_s)}{2-2\mathrm{sinc}^2(\phi_s)+\mathrm{sinc}(2\phi_s)}\,,\\
B_{1,1}^{(2)} &= \frac{\alpha^2}{64\phi_s^2}\frac{2}{\alpha^2}\left[(2-2\mathrm{sinc}^2(\phi_s)+\mathrm{sinc}(2\phi_s))^{-1}+(2-\mathrm{sinc}(2\phi_s))^{-1}\right],\\
B_{1,-1}^{(2)} &= \frac{\alpha^2}{64\phi_s^2}\frac{2}{\alpha^2}\left[(2-2\mathrm{sinc}^2(\phi_s)+\mathrm{sinc}(2\phi_s))^{-1}-(2-\mathrm{sinc}(2\phi_s))^{-1}\right],\\
B_{1,0}^{(2)} &= -\frac{\alpha^2}{64\phi_s^2}\frac{8}{\alpha}\frac{\mathrm{sinc}(\phi_s)}{2-2\mathrm{sinc}^2(\phi_s)+\mathrm{sinc}(2\phi_s)}\,,
\end{aligned}$$

and hence,

$$\begin{aligned}
\hat{h}_0^{\mathrm{est},(2)} &= \hat{h}_0 + O(\alpha^2)\,,\\
\hat{h}_1^{\mathrm{est},(2)} &= \hat{h}_1 + O(\alpha)\,.
\end{aligned}$$

We have improved the accuracy of the estimate of $\hat{h}_0$ with respect to the approximation error in $O(\alpha)$ in (37), and we have derived an estimation of $\hat{h}_1$ of the same accuracy as the estimation of $\hat{h}_0$ in (37).

It is of course possible to implement this method beyond $p=1$ and to identify the matrix $B^{(p+1)}=(B^{(p+1)}_{j,l})_{j=0,\dots,p,l=-p,\dots,p}$ so that

$$\hat{h}_j^{\mathrm{est},(p+1)} = \varepsilon^{-2}\sum_{l=-p}^{p} B^{(p+1)}_{j,l}(\alpha)(\mathcal{Q}^\star \hat{a}^{\mathrm{mes}})_l\,, \qquad j=0,\dots,p\,,$$

and

$$\hat{h}_j^{\mathrm{est},(p+1)} = \hat{h}_j + O(\alpha^{p+1-j}), \qquad j=0,\dots,p\,. \tag{39}$$

Assuming that $\hat{h}_j=0$ for $j=-(p-1),\dots,(p-1)$, we obtain

$$(\mathcal{Q}^\star \hat{a}^{\mathrm{mes}})_p = 64\varepsilon^2\phi_s^2\alpha^{2p-2}\Big[(p-\frac{1}{2})\hat{h}_p + \frac{1}{4}\mathrm{sinc}(2p\phi_s)\hat{h}_{-p} + O(\alpha)\Big]\,,$$

and therefore we can estimate $\hat{h}_p$ by the formula

$$\hat{h}_p^{\mathrm{est}} = \varepsilon^{-2}\Big[B_{p,p}(\alpha)(\mathcal{Q}^\star \hat{a}^{\mathrm{mes}})_p + B_{p,-p}(\alpha)(\mathcal{Q}^\star \hat{a}^{\mathrm{mes}})_{-p}\Big]\,, \tag{40}$$

where

$$\begin{aligned} B_{p,p} &= \frac{\alpha^{2-2p}}{64\phi_s^2}(p-1/2)\Big((p-\frac{1}{2})^2 - \frac{1}{16}\mathrm{sinc}^2(2p\phi_s)\Big)^{-1}\,,\\ B_{p,-p} &= -\frac{\alpha^{2-2p}}{64\phi_s^2}\frac{\mathrm{sinc}(2p\phi_s)}{4}\Big((p-\frac{1}{2})^2 - \frac{1}{16}\mathrm{sinc}^2(2p\phi_s)\Big)^{-1}\,. \end{aligned}$$

As before, the estimation of the pth mode is a first-order estimation in α:

$$\hat{h}_p^{\mathrm{est}} = \hat{h}_p + O(\alpha)\,.$$

5.2. **Noise Constrained Resolution.** In the general case $\phi_r,\phi_s\in(0,\pi]$, we have using (13) and (16)

$$\begin{aligned} \mathbb{E}\Big[|(\mathcal{Q}^\star\hat{W})_p|^2\Big] &= (\mathcal{Q}^\star\mathcal{Q}\mathbf{1}_p)_p\\ &= \varepsilon^2\frac{\phi_s^2\phi_r^2}{\pi^4}\sum_{j,j'=-\infty}^{\infty}\mathrm{sinc}((j-j')\phi_r)\mathrm{sinc}((j-j')\phi_s)e^{i(j-j')\phi_c}\\ &\quad\times c_{p-j,j}(\alpha)c_{p-j',j'}(\alpha)\,. \end{aligned}$$

In the regime $\alpha\to 0$, we find

$$\begin{aligned} \mathbb{E}[|(\mathcal{Q}^\star\hat{W})_0|^2] &= \varepsilon^2\frac{4\phi_s^2\phi_r^2}{\pi^2}\alpha^{-2}\big[1+O(\alpha)\big]\,,\\ \mathbb{E}[|(\mathcal{Q}^\star\hat{W})_1|^2] &= \varepsilon^2\frac{32\phi_s^2\phi_r^2}{\pi^2}\Big[\mathrm{sinc}(\phi_r)\mathrm{sinc}(\phi_s)\cos(\phi_c)+1\Big]\big[1+O(\alpha)\big]\,, \end{aligned}$$

and

$$\begin{aligned} \mathbb{E}[|(\mathcal{Q}^\star\hat{W})_p|^2] &= \varepsilon^2\frac{32\phi_s^2\phi_r^2}{\pi^2}\alpha^{2p-2}\Big[\mathrm{sinc}(p\phi_r)\mathrm{sinc}(p\phi_s)\cos(p\phi_c)\\ &\quad +4\sum_{j=1}^{p-1}(p-j)\mathrm{sinc}(j\phi_r)\mathrm{sinc}(j\phi_s)\cos(j\phi_c)+(2p-1)\Big]\big[1+O(\alpha)\big]\,. \end{aligned} \tag{41}$$

To be complete, we should add that the coefficients are correlated. For instance

$$\mathbb{E}[(\mathcal{Q}^\star\hat{W})_1\overline{(\mathcal{Q}^\star\hat{W})_0}] = \varepsilon^2\frac{8\phi_s^2\phi_r^2}{\pi^2}\alpha^{-1}\Big[\mathrm{sinc}(\phi_s)+\mathrm{sinc}(\phi_r)e^{-i\phi_c}\Big]\big[1+O(\alpha)\big]\,.$$

Moreover, for any $p \geq 1$, we have

$$\mathbb{E}[(\mathcal{Q}^\star \hat{W})_p \overline{(\mathcal{Q}^\star \hat{W})_{-p}}] = \varepsilon^2 \frac{16\phi_s^2\phi_r^2}{\pi^2}\alpha^{2p-2}\Big[\mathrm{sinc}(2p\phi_s) + \mathrm{sinc}(2p\phi_r)e^{-2ip\phi_c} + 4\sum_{j=1}^{2p-1}\Big(j \wedge (2p-j) \wedge (p-\frac{1}{2})\Big)\mathrm{sinc}((j-2p)\phi_r)\mathrm{sinc}(j\phi_s)e^{i(j-2p)\phi_c}\Big]\big[1+O(\alpha)\big]\,, \tag{42}$$

where $a \wedge b$ is a shorthand for $\min(a,b)$.

We now come back to the case of full receiver and partial source apertures $\phi_r = \pi$, $\phi_s \in (0,\pi]$. When we use estimator (27), the error due to the measurement noise is given by

$$\hat{e}_p^{\mathrm{est}} = \hat{h}_p^{\mathrm{est}} - \mathbb{E}[\hat{h}_p^{\mathrm{est}}] = \varepsilon^{-2}\sigma \sum_{r=-\infty}^{\infty} B_{p,r}(\alpha)(\mathcal{Q}^\star \hat{W})_r\,.$$

When the receiver aperture is full so that $\phi_r = \pi$, we have the following important results:

(i) If we estimate $\hat{h}_0$ with estimator (36), then the measurement error has variance

$$\mathbb{E}[|\hat{e}_0^{\mathrm{est}}|^2] = \frac{\sigma^2}{\varepsilon^2}\frac{\alpha^2}{4\phi_s^2}\,, \tag{43}$$

while the approximation error is of order $O(\alpha)$.

(ii) If we estimate $\hat{h}_0$ with estimator (38), then the measurement error has variance

$$\mathbb{E}[|\hat{e}_0^{\mathrm{est}}|^2] = \frac{\sigma^2}{\varepsilon^2}\frac{\alpha^2}{4\phi_s^2}\frac{2+\mathrm{sinc}(2\phi_s)}{2-2\mathrm{sinc}^2(\phi_s)+\mathrm{sinc}(2\phi_s)}\,, \tag{44}$$

while the approximation error is of order $O(\alpha^2)$. By comparing (43) and (44) we can see that we have a significant gain in the approximation error without losing stability.

(iii) If we estimate $\hat{h}_1$ with estimator (38), then the measurement error has variance

$$\mathbb{E}[|\hat{e}_1^{\mathrm{est}}|^2] = \frac{\sigma^2}{\varepsilon^2}\frac{1}{32\phi_s^2}\Big(\frac{2+\mathrm{sinc}(2\phi_s)}{\big(2-2\mathrm{sinc}^2(\phi_s)+\mathrm{sinc}(2\phi_s)\big)^2} + \frac{1}{2-\mathrm{sinc}(2\phi_s)}\Big)\,, \tag{45}$$

while the approximation error is of order $O(\alpha)$. By comparing (44) and (45) we can see that the estimations of the high modes are more sensitive to measurement noise than those of the low modes.

(iv) More generally, if we estimate $\hat{h}_p$ with (40), then we find that

$$\mathbb{E}[|\hat{e}_p^{\mathrm{est}}|^2] = \frac{\sigma^2}{\varepsilon^2}\alpha^{2-2p}\frac{(2p-1)}{32\phi_s^2\Big((2p-1)^2 - \frac{1}{4}\mathrm{sinc}^2(2p\phi_s)\Big)}\,, \tag{46}$$

while the approximation error, $\hat{h}_p^{\mathrm{est}} - \hat{h}_p$, is of order $O(\alpha)$.

This yields the following proposition.

Proposition 5.1. *Suppose that $\alpha \ll 1$ and $\phi_r = \pi$. Let* SNR *be defined by (18). It is possible to estimate the zero-th order Fourier mode $\hat{h}_0$ if*

$$\frac{\alpha^2}{4\phi_s^2} < \mathrm{SNR}\,.$$

Let $p_{\max}$ be the highest Fourier mode of h that can be resolved. The sufficient resolution constraint

$$\frac{1}{2p_{\max}-1}\frac{\alpha^{2-2p_{\max}}}{32\phi_s^2} < \mathrm{SNR}$$

holds.

When $\phi_s = \pi$ Proposition 5.1 gives the same result as (22). Note that the estimation of the zero-th order Fourier mode corresponds to the estimation of the volume of the perturbed inclusion. The estimation of the first Fourier mode corresponds to the estimation of the eccentricity of the equivalent ellipse which gives the same first-order boundary perturbations. The higher modes correspond to more refined details. Proposition 5.1 shows that for large SNR we have

$$p_{\max} < \frac{\log(\mathrm{SNR})}{-2\log(\alpha)}\,.$$

Thus, the mode number bound becomes small for small inclusions. However, given the unperturbed inclusion radius, α, we find that the following resolution measure defined by

$$\lambda^\star := \frac{2\pi\alpha}{p_{\max}}\,, \tag{47}$$

is approximately

$$\lambda^\star \sim -\frac{4\pi\alpha\log(\alpha)}{\log(\mathrm{SNR})}\,,$$

and therefore, the resolution improves for small inclusions due to the reduction in scale for fixed p with reduced radius α.

5.3. **The Case of Partial Source and Partial Receiver.** In this subsection we consider the case when the receiver aperture and the source aperture are partial, so that $\phi_r, \phi_s \in (0,\pi)$. In the absence of measurement noise, we have

$$(\mathcal{Q}^\star\hat{a}^{\mathrm{mes}})_p = \frac{\varepsilon^2\phi_s^2\phi_r^2}{\pi^4}\sum_{j,m,n=-\infty}^{\infty} e^{i(n+j-p)\phi_c}\mathrm{sinc}(\phi_s(j-m))\mathrm{sinc}(\phi_r(j+n-p)) \times c_{p-j,j}(\alpha)c_{n,m}(\alpha)\hat{h}_{n+m}\,.$$

When $\alpha \ll 1$, we can readily get

$$\begin{aligned}
(\mathcal{Q}^\star\hat{a}^{\mathrm{mes}})_0 &= \frac{64\varepsilon^2\phi_s^2\phi_r^2}{\pi^2\alpha^2}\Big[\frac{1}{16}\hat{h}_0 + \frac{\alpha}{8}(e^{i\phi_c}\mathrm{sinc}(\phi_r)+\mathrm{sinc}(\phi_s))\hat{h}_1 \\
&\quad + \frac{\alpha}{8}(e^{-i\phi_c}\mathrm{sinc}(\phi_r)+\mathrm{sinc}(\phi_s))\hat{h}_{-1} + O(\alpha^2)\Big]\,, \\
(\mathcal{Q}^\star\hat{a}^{\mathrm{mes}})_1 &= \frac{64\varepsilon^2\phi_s^2\phi_r^2}{\pi^2\alpha^2}\Big[\frac{\alpha^2}{2}\big(1+\mathrm{sinc}(\phi_r)\mathrm{sinc}(\phi_s)\cos(\phi_c)\big)\hat{h}_1 \\
&\quad + \frac{\alpha^2}{4}\big(\mathrm{sinc}(2\phi_s)+2\mathrm{sinc}(\phi_s)\mathrm{sinc}(\phi_r)e^{-i\phi_c}+\mathrm{sinc}(2\phi_r)e^{-2i\phi_c}\big)\hat{h}_{-1} \\
&\quad + \frac{\alpha}{8}\big(\mathrm{sinc}(\phi_s)+\mathrm{sinc}(\phi_r)e^{-i\phi_c}\big)\hat{h}_0 + O(\alpha^3)\Big]\,,
\end{aligned}$$

and

$$(\mathcal{Q}^\star\hat{a}^{\mathrm{mes}})_{-1} = \overline{(\mathcal{Q}^\star\hat{a}^{\mathrm{mes}})_1}, \quad (\mathcal{Q}^\star\hat{a}^{\mathrm{mes}})_p = O(\alpha^{p-2}) \qquad \text{for all } p \geq 2.$$

Similarly, if $\hat{h}_j = 0$ for $|j| \leq p-1$, then

$$\begin{aligned}
(\mathcal{Q}^\star \hat{a}^{\rm mes})_p &= \varepsilon^2 \frac{64\phi_s^2\phi_r^2}{\pi^2}\alpha^{2p-2}\Big[Q_{p,p}\hat{h}_p + Q_{p,-p}\hat{h}_{-p}\Big]\big[1+O(\alpha)\big]\,,\\
Q_{p,p} &= \frac{1}{2}{\rm sinc}(p\phi_r){\rm sinc}(p\phi_s)\cos(p\phi_c)\\
&\quad +2\sum_{j=1}^{p-1}(p-j){\rm sinc}(j\phi_r){\rm sinc}(j\phi_s)\cos(j\phi_c) + (p-\frac{1}{2})\,,\\
Q_{p,-p} &= \frac{1}{4}{\rm sinc}(2p\phi_r)e^{-2ip\phi_c} + \frac{1}{4}{\rm sinc}(2p\phi_s)\\
&\quad + \sum_{j=1}^{2p-1} j\wedge(2p-j)\wedge(p-\frac{1}{2}){\rm sinc}((j-2p)\phi_r){\rm sinc}(j\phi_s)e^{i(j-2p)\phi_c}\,.
\end{aligned}$$

Using (41) and (42) this gives the following proposition.

Proposition 5.2. *Suppose that $\alpha \ll 1$. Let* SNR *be defined by (18). It is possible to estimate the zero-th order Fourier mode $\hat{h}_0$ if*

$$\frac{\pi^2\alpha^2}{4\phi_s^2\phi_r^2} < {\rm SNR}\,.$$

Let $p_{\max}$ be the highest Fourier mode of h that can be resolved. The sufficient resolution constraint

$$\frac{\pi^2}{32\phi_s^2\phi_r^2}\frac{\alpha^{2-2p_{\max}}}{2p_{\max}-1} < {\rm SNR}$$

holds.

We see from Proposition 5.2 that, given SNR and α, the mode number bound becomes small for small apertures of the source and receiver arrays, or equivalently, the resolution measure, $\lambda^\star$ defined by (47), becomes large. Moreover, the fact that the two arrays are superposed plays no role in the case of small inclusions, only the apertures are important, in contrast to the case of an inclusion with a large diameter studied in Section 4.

6. Conclusion

In this paper we have established resolution and stability estimates for the linearized conductivity problem with limited-view data in the presence of measurement noise. We have shown that in the shallow probing regime we can resolve for any fixed SNR a sufficiently shallow perimeter perturbation of the conductivity inclusion on the overlap of the source and receiver apertures. This has been done using a filter with a diagonal scaling. In the general case, such a filter would not lead correct images. In the deep probing regime, we have provided a matrix filter in order to estimate the lowest modes of the shape perturbations. We emphasize that the conclusions of this paper as those of [6] hold only under the assumption that the noise is measurement noise. For medium noise or clutter, the situation is quite different. This will be the subject of a forthcoming investigation. Another challenging problem is to extend the present resolution analysis to acoustic and elastic wave propagation problems. In view of [4], [5], and [7] similar resolution estimations may be expected to hold in the acoustic and elastic cases.

References

[1] M. Abramowitz and I. Stegun (editors), *Handbook of Mathematical Functions*, National Bureau of Standards, Washington D.C., 1964.

[2] G. Alessandrini, Open issues of stability for the inverse conductivity problem, J. Inverse Ill-Posed Probl., 15 (2007), 451–460.

[3] G. Alessandrini and M. Di Cristo, Stable determination of an inclusion by boundary measurements, SIAM J. Math. Anal., 37 (2005), 200–217.

[4] H. Ammari, E. Beretta, E. Francini, H. Kang, and M. Lim, Optimization algorithm for reconstructing interface changes of a conductivity inclusion from modal measurements, Math. Comp., 79 (2010), 1757–1777.

[5] H. Ammari, E. Beretta, E. Francini, H. Kang, and M. Lim, Reconstruction of small interface changes of an inclusion from modal measurements II: The elastic case, J. Math. Pures Appl., 94 (2010), 322–339.

[6] H. Ammari, J. Garnier, and K. Sølna, Resolution and stability analysis in full-aperture, linearized conductivity and wave imaging, Proc. Amer. Math. Soc., to appear.

[7] H. Ammari, H. Kang, and H. Lee, *Layer Potential Techniques in Spectral Analysis*, Mathematical Surveys and Monographs, Vol. 153, American Mathematical Society, Providence, RI, 2009.

[8] H. Ammari, H. Kang, M. Lim, and H. Zribi, Conductivity Interface Problems. Part I: Small perturbations of an Interface, Trans. Amer. Math. Soc., 362, 2435-2449, 2010.

[9] H. Ammari, O. Kwon, J. K. Seo, and E. J. Woo, T-scan electrical impedance imaging system for anomaly detection, SIAM J. Appl. Math., 65 (2005), 252–266.

[10] K. Astala and L. Päivärinta, Calderón's inverse conductivity problem in the plane, Ann. Math., 163 (2006), 265–299.

[11] A. Beck and M. Teboulle, A fast iterative shrinkage-thresholding algorithm for linear inverse problems, SIAM J. Imaging Sci., 2 (2009), 183–202.

[12] L. Borcea, Electrical impedance tomography, Inverse problems, 18 (2002), R99–R136.

[13] G. Boverman, T.-J. Kao, D. Isaacson, and G. J. Saulnier, An implementation of Calderón's method for 3-D limited-view EIT, IEEE Trans. Med. Imaging, 28 (2009), 1073–1082.

[14] I. Daubechies, M. Defrise, and C. De Mol, An iterative thresholding algorithm for linear inverse problems with a sparsity constraint, Comm. Pure Appl. Math., 57 (2004), 1413–1457.

[15] D. Dos Santos Ferreira, C. Kenig, J. Sjöstrand, and G. Uhlmann, On the linearized local Calderón problem, Math. Res. Lett., 16 (2009), 955–970.

[16] A. Friedman, Detection of mines by electric measurements, SIAM J. Appl. Math., 47 (1987), 201–212.

[17] T. Ide, H. Isozaki, S. Nakata, S. Siltanen, and G. Uhlmann, Probing for electrical inclusions with complex spherical waves, Comm. Pure Appl. Math., 60 (2007), 1415–1442.

[18] O. Y. Imanuvilov, G. Uhlmann, and M. Yamamoto, The Calderón problem with partial data in two dimensions, J. Amer. Math. Soc., 23 (2010), 655–691.

[19] V. Isakov, On uniqueness of recovery of a discontinuous conductivity coefficient, Comm. Pure Appl. Math., 41 (1988), 865–877.

[20] V. Isakov, The inverse conductivity problem with limited data and applications, J. Phys.: Conf. Series, 73 (2007), 012011.

[21] P. Kearey, M. Brooks, and I. Hill, *An Introduction to Geophysical Exploration*, 3rd edition, Blackwell Science, Oxford, 2002.

[22] C. Kenig, J. Sjöstrand, and G. Uhlmann, The Calderón problem with partial data, Annals of Math., 165 (2007), 567–591.

[23] O. Kwon, J. R. Yoon, J. K. Seo, E. J. Woo, and Y. G. Cho, Estimation of anomaly location and size using impedance tomography, IEEE Trans. Biomed. Engr., 50 (2003), 89–96.

[24] G. Uhlmann, Calderón's problem and electrical impedance tomography, Inverse Problems, 25 (2009), 123011.

Department of Mathematics and Applications, Ecole Normale Supérieure, 45 Rue d'Ulm, 75005 Paris, France.
E-mail address: habib.ammari@ens.fr

Laboratoire de Probabilités et Modèles Aléatoires & Laboratoire Jacques-Louis Lions, Université Paris VII, 75205 Paris Cedex 13, France.
E-mail address: garnier@math.univ-paris-diderot.fr

Department of Mathematics, University of California, Irvine, CA 92697
E-mail address: ksolna@math.uci.edu